



UPPSALA  
UNIVERSITET

Independent Project at the Department of Earth Sciences  
Självständigt arbete vid Institutionen för geovetenskaper  
2021:7

# An Overview of State-of-the-art Hydraulic Conductivity Measurements in Coarse Grained Materials

En översikt över toppmoderna mätmetoder för  
hydraulisk konduktivitet i grovkorniga material

Jakob Andrén

DEPARTMENT OF  
EARTH SCIENCES

INSTITUTIONEN FÖR  
GEOVETENSKAPER



# An Overview of State-of-the-art Hydraulic Conductivity Measurements in Coarse Grained Materials

En översikt över toppmoderna mätmetoder för  
hydraulisk konduktivitet i grovkorniga material

Jakob Andrén

Copyright © Jakob Andrén

Published at Department of Earth Sciences, Uppsala University ([www.geo.uu.se](http://www.geo.uu.se)),  
Uppsala, 2021

# Abstract

## An Overview of State-of-the-art Hydraulic Conductivity Measurements in Coarse Grained Materials

*Jakob Andrén*

Embankment dams are made from soil materials of varying sizes and widely used all over the world. When constructing these, knowing the hydraulic conductivity ( $K$ ) of the soil materials is a key parameter in order to construct safe embankment dams. A knowledge gap regarding  $K$  measurements in coarse grained soils has been identified. This thesis aims to provide a theoretical overview of present day state-of-the-art methods for measuring hydraulic conductivity and the controlling characteristics for  $K$ . Coarse grained soils refers to a soil with the coarsest grain fraction being  $\geq 20$  mm and/or have a  $K \geq 10^{-4}$  m/s.

It was found that the fixed wall permeameter is the most suitable laboratory method. In the field, it is possible to estimate  $K$  using tracer methods, these however show more potential for leakage pathway detection. Common for all  $K$  measurement methods are the controlling characteristics of  $K$ , grain size distribution, pore geometry, degree of compaction, particle movement and flow regime. These need to be considered when testing to produce useful measurements. If the relationship between flow velocity and hydraulic head is non-linear, Darcy's law is not valid for calculating  $K$ .

**Keywords:** hydraulic conductivity, permeability, embankment dam, coarse grained, flow regime

*Independent Project in Earth Science, IGV029, 15 credits, 2021*

*Supervisors: Johan Lagerlund & Benjamin Fischer*

*Department of Earth Sciences, Uppsala University, Villavägen 16, SE-752 36 Uppsala  
([www.geo.uu.se](http://www.geo.uu.se))*

*The whole document is available at [www.diva-portal.org](http://www.diva-portal.org)*

# Sammanfattning

## En översikt över toppmoderna mätmetoder för hydraulisk konduktivitet i grovkorniga material

*Jakob Andrén*

Fyllnadsdammar är uppbyggda av jord och sprängsten av olika storlekar och finns över hela världen. Att känna till den hydrauliska konduktiviteten ( $K$ ) av de olika lagren är viktigt för att kunna bygga dessa på ett säkert och hållbart sätt. Det har identifierats en bristande kunskap angående  $K$  mätningar i grovkorniga jord- och stenmaterial. Målet med denna uppsats är att presentera en teoretisk översikt av den senaste kunskapen inom  $K$  mätningar i grovkorniga jord- och stenmaterial och vilka egenskaper som avgör ett materials  $K$ . Grovkorniga jord- och stenmaterial syftar till material där den grövsta kornstorleken är  $\geq 20$  mm och/eller har ett  $K \geq 10^{-4}$  m/s.

För laboratorie mätningar är en permeameter med en solid vägg den mest lämpliga metoden. För fältmätningar är det möjligt att mäta  $K$  med hjälp av spårämnen, men dessa har mer potential för att upptäcka läckage vägar i fyllnadsdammar. De faktorer som avgör ett materials  $K$  är kornstorleksfördelningen, geometrin av porerna, graden av kompaktering, partikelrörelse och flödestyp. För att producera mätningar som är användbara behöver dessa faktorer kontrolleras. Om sambandet mellan hydrauliskt huvud och flödes hastighet är icke linjärt kan  $K$  inte beräknas genom Darcy's lag.

**Nyckelord:** Hydraulisk konduktivitetsmätning, permeabilitet, fyllnadsdamm, grovkorniga material, flödesregim

*Självständigt arbete i geovetenskap, 1GV029, 15 hp, 2021*

*Handledare: Johan Lagerlund & Benjamin Fischer*

*Institutionen för geovetenskaper, Uppsala universitet, Villavägen 16, 752 36 Uppsala*

*([www.geo.uu.se](http://www.geo.uu.se))*

*Hela publikationen finns tillgänglig på [www.diva-portal.org](http://www.diva-portal.org)*

## Acknowledgments

I would like to give a special thank you to Johan Lagerlund from Vattenfall. Partly for supplying the question for this thesis but primarily for his outstanding support and feedback. At several occasions receiving a report absolutely full of comments, several being supportive of what is written or explaining his chain of thought about a topic. This is truly unique for my time as a student, very appreciated and has enabled me to develop my writing much more than I otherwise would have.

I would also like to thank Benjamin Fischer for his support, expertise and guidance in the world of tracer methods and lengthy meetings regarding future work.

## List of symbols

$K$  = hydraulic conductivity (length/time)  
 $K_s$  = saturated hydraulic conductivity (length/time)  
 $k$  = intrinsic permeability (dimensionless)  
 $\mu$  = fluid viscosity ( $\text{m}^2/\text{s}$ )  
 $\eta_{\text{fl}}$  = dynamic fluid viscosity ( $\text{Pa} \times \text{s}$  or  $\text{kg}/\text{s} \times \text{m}$ )  
 $\nu$  = kinematic viscosity ( $\text{m}^2/\text{s}$ )  
 $\rho$  = fluid density ( $\text{kg}/\text{m}^3$ )  
 $g$  = gravitational acceleration ( $\text{m}/\text{s}^2$ )  
 $i$  = hydraulic gradient (dimensionless)  
 $p$  = pressure head (m)  
 $z$  = elevation head (m)  
 $h$  = hydraulic head (m)  
 $l$  = distance two measuring points along a streamline (m)  
 $d$  = diameter (m, mm)  
 $d\text{-max}$  = the largest grain diameter in a sample (m, mm)  
 $Q$  = discharge (volume/time)  
 $A$  = area ( $\text{m}^2$ )  
 $Re$  = Reynolds number (dimensionless)  
 $Re_{\text{pore}}$  = Reynolds number based on pores (dimensionless)  
 $v$  = mean fluid velocity (m/s)  
 $V$  = bulk velocity (m/s)  
 $m$  = hydraulic mean radius with no wall effect (m, mm)  
 $n$  = porosity (dimensionless)  
 $e$  = void ratio (dimensionless)  
 $A_{VS}$  = volume specific surface area ( $\text{m}^2/\text{kg}$ )



# Table of contents

<b>1. Introduction</b>	<b>1</b>
1.1 Embankment dams	1
1.2 Defining hydraulic conductivity	3
1.3 The primary determining characteristic of hydraulic conductivity	5
1.4 Tracers	7
1.5 Research questions	8
<b>2. Method</b>	<b>8</b>
2.1 Demarcation	9
<b>3. Results</b>	<b>9</b>
3.1 Laboratory methods	9
3.2 Field methods	13
<b>4. Discussion</b>	<b>20</b>
4.1 Laboratory methods suitable for coarse grained materials	21
4.2 Field methods suitable for coarse grained materials	22
4.3 The primary determining characteristic of hydraulic conductivity	23
<b>5. Topics for future work</b>	<b>23</b>
<b>6. Conclusion &amp; recommendations</b>	<b>23</b>
<b>References</b>	<b>24</b>
Internet resources	26
Personal communication	26



# 1. Introduction

Embankment dams have been used for thousands of years to control water for flood control, irrigation and today to produce electricity. They are structures built up of several layers of rock and soil (“What is Embankment Dam?,” 2018). Due to the nature of dams holding back water, the danger from a dam failing is not from the dam collapsing and causing damage like a building would, but from the stored energy in the water rushing downstream. Even a relatively small dam can have deadly consequences when collapsing, as witnessed 1977 when the Kelly Barnes dam broke. The dam measured roughly 12 x 120 m and when it collapsed it released a water flow estimated at 680 m<sup>3</sup>/s, killing 39 people downstream (Filters for Embankment Dams, 2011).

The primary cause of dam failure is from internal erosion. Erosion is caused by water moving through the dam faster than was intended. As a result, particles are transported, causing erosion, affecting the structural integrity of the dam (Ferdos et al., 2015). Embankment dams are designed to leak a certain amount and be able to withstand a certain through flow, also called drainage capacity, without failing. Certain zones of the dam need to allow more water through than others. Hydraulic conductivity,  $K$ , is one of the key parameters used when designing an embankment dam (Statens vattenfallsverk, 1988).  $K$ , refers to a material's resistance towards water flowing through it and is measured in meters per second. A higher  $K$  allows for more water to move at a faster velocity through a material (Hölting and Coldewey, 2019). There is no set definition for coarse grained materials, in this thesis coarse grained refers to a material with the coarsest grain fraction being  $\geq 20$  mm and/or have a  $K \geq 10^{-4}$  m/s.

This study is being conducted because no overviews of  $K$  measurements in coarse grained materials have been found and the Swedish dam industry saw a need to fill potential knowledge gaps. Several industry standards exist such as Australian standards, AS, ASTM and ISO that cover coarse grained materials but only ISO standards were directly accessed during this study. ISO standards did not present a sufficient overview of the measurement methods or the theoretical background to the recommendations made in the standards.

## 1.1 Embankment dams

An embankment dam refers to a dam primarily constructed out of compacted soil and rock, built up by several layers of different grain sizes and properties, figure 1 (Statens vattenfallsverk, 1988).

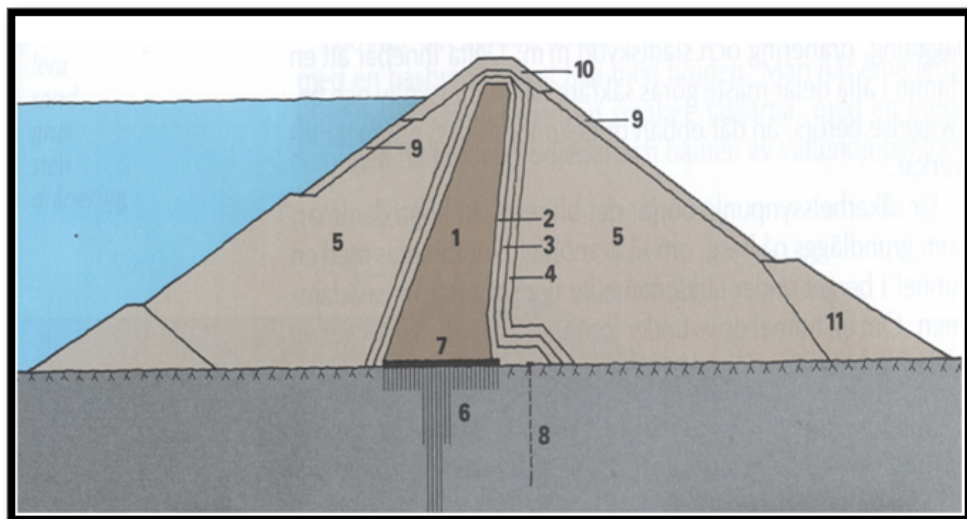


**Figure 1.** A schematic cross-section of a high embankment dam ( $> 15$ m), 1-the core, 2-4-filters, 5-support rockfill, 6- bedrock injection, 7-concrete foundation, 8-fiterwell, 9-10-erosion protection and 11-dam toe (Statens vattenfallsverk, 1988 bild 5.1).

Zones 5 and 9-11 consist of the coarse soil material referred to in this thesis. The list below presents more detailed explanations to the different layers in figure 1:

1. The core acts as a nearly impermeable barrier in the dam with dimensions depending on the height of the dam, strength of the foundation and underlying material, width of the dam, the material used and more. One soil that can be used is till (moraine), if it has a permeability of  $3 \times 10^{-7}$  -  $3 \times 10^{-9}$  m/s and a fine soil content ( $< 0.06$  mm) of 15-40 %, figure 2.

2-4. Filters of increasing grain size. These keep the finer material in the core in place by having a pore size small enough to keep finer material from washing out, this is called filter criterion. The filters have a limited grain size distribution, so as not to separate during construction. An example of these grain sizes can be seen in figure 2.

5. Support rockfill, acts to keep the core and filters in place, figure 2. In the contact with the filter layers the pore size needs to meet the filter criterion. If the filters and the core are damaged the support rockfill should have a high enough  $K$  to allow a lot of water through, without deforming and breaking. Thus preventing a complete collapse of the dam.

6. The bedrock injection serves to seal the bedrock from water, maintain a steady water pressure in the bedrock below the dam and strengthen the bedrock to withstand the weight of the dam without deforming.

7. The concrete foundation acts as a load distribution, connecting the dam core to the bedrock as well as a seal for the bedrock injection to build pressure against and achieve sealing. The foundation is anchored into the bedrock with bolts.

8. The filterwell collects seepage water from the foundation to reduce build up of pore pressure from the water. High pore pressure reduces the stability of the material and therefore needs to be controlled.

9-10. Protection from erosion from waves, rain, ice and flooding. These sections are constructed out of carefully placed blocks for maximum strength, and a contact pore size small enough to meet the filter criterion.

11. The dam toe supplies extra support for the dam downstream where the water leaks out (Vattenfall 1988).

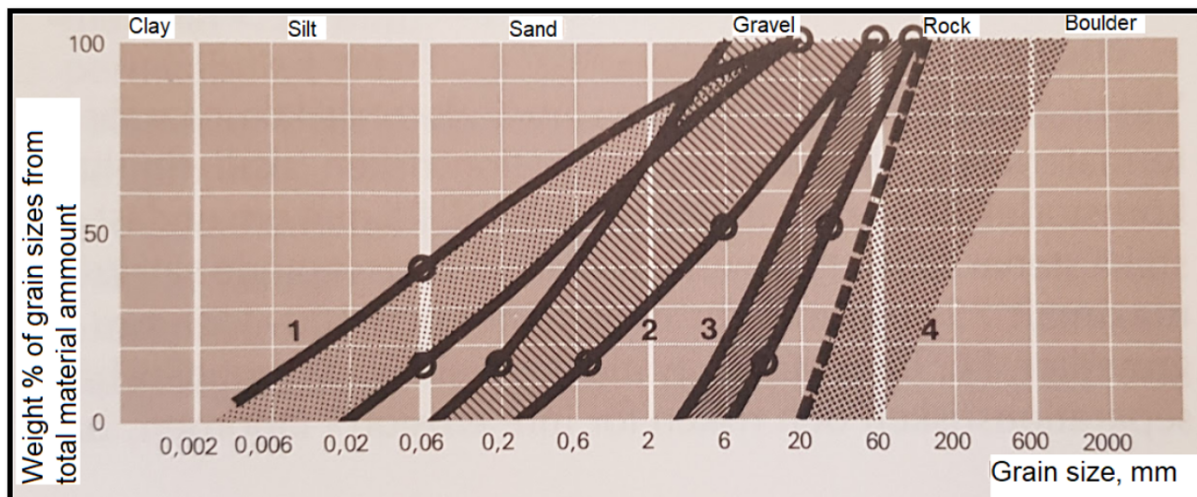


**Figure 2.** Grain size distribution curves example for an embankment dam. 1-The core, 2-3 filters and 4-support rockfill (translated from Statens vattenfallsverk, 1988 bild 6.5)

When designing an embankment dam, the thickness of the layers and their grain size distribution are determined in order to meet the requirements for that layer as detailed above. The support rockfill and outermost layers of coarse rock needs to allow a lot of water through in case of damage to the core, while maintaining its stability. The  $K$  is a key parameter to determine the composition of these layers in order to remain stable under high hydraulic load (Statens vattenfallsverk, 1988).

## 1.2 Defining hydraulic conductivity

The concepts hydraulic conductivity,  $K$ , saturated hydraulic conductivity,  $K_s$ , permeability and intrinsic permeability are all important to understand and specify when discussing  $K$  measurements. These can sometimes be used interchangeably (Chesworth et al., 2021; “Soil Survey Technical Note 6 | NRCS Soils,” n.d.), or with important differences. Below are the definitions used in this thesis.

### 1.2.1 Hydraulic gradient & hydraulic head:

Hydraulic gradient,  $i$ , can be defined as the driving force behind water movement. If there is no hydraulic gradient, the water will be in equilibrium and not move. Hydraulic head,  $h$  (m), is the liquid pressure above a certain horizontal reference plane and the hydraulic gradient is the difference between two hydraulic heads divided by the length travelled along a streamline,  $l$  (m), equation 1 (eq 1) (Hölting and Coldewey, 2019; Marshak, 2015).

$$(1) \quad h = \frac{(h_1 - h_2)}{l}$$

Hydraulic head is divided into elevation head,  $z$  (m), and pressure head,  $p$  (m), and the full equation for hydraulic gradient,  $i$  (dimensionless), can be written according to (eq 2), figure 3 (Chesworth et al., 2021).

$$(2) \quad i = \frac{(p_1 + z_1) - (p_2 + z_2)}{l}$$

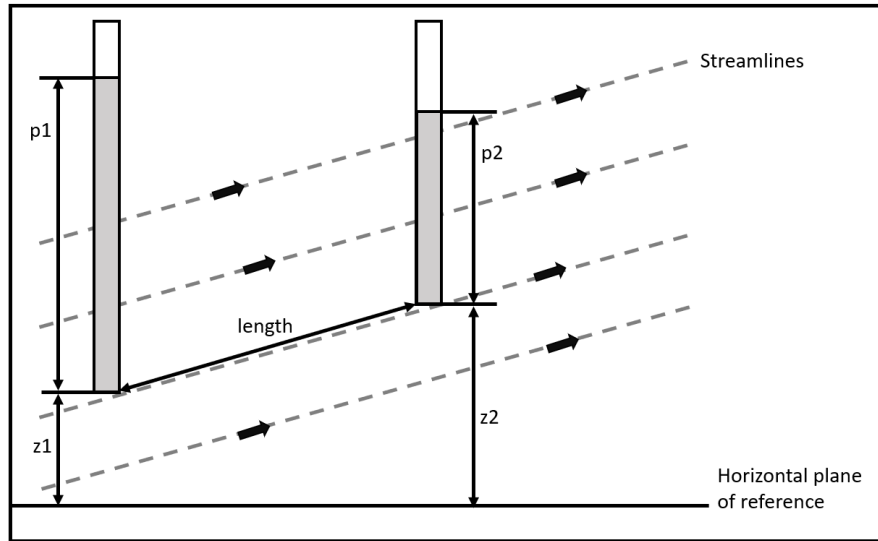


**Figure 3.** Pressure heads,  $p$ , and elevation heads,  $z$ , the black bottom line is a horizontal plane of reference, the dotted lines are streamlines and length refers to the length along the streamline (adapted from Chesworth et al., 2021).

### 1.2.2 Darcy's law:

Darcy's law states that for a certain hydraulic gradient and a specific cross sectional area,  $A$  (m<sup>2</sup>), the discharge,  $Q$  (volume/time), will depend on the hydraulic conductivity,  $K$  (length/time), (eq 3) (Marshak, 2015). Bear, n.d. state that Darcy's law is a linear relationship between discharge and hydraulic gradient and is only valid for laminar flow.

$$(3) \quad Q = \frac{K \times A(h_1 - h_2)}{l}$$

The  $K$ -value describes how much resistance the material has to water flowing through it. It is not only dependent on the factors in (eq 3) but also the viscosity of the fluid,  $\mu$  (m<sup>2</sup>/s), the density of the fluid,  $p$  (kg/m<sup>3</sup>), the acceleration due to gravity,  $g$  (m/s<sup>2</sup>), and the intrinsic permeability,  $k$  (dimensionless). Intrinsic permeability,  $k$ , does not account for direction or gradient but is a property of the material based only on the geometry of the pores, (eq 4), (Chesworth et al., 2021; Hölting and Coldewey, 2019).

$$(4) \quad k = \frac{K \times \mu}{p \times g}$$

### 1.2.3 Saturated hydraulic conductivity & permeability:

The above equations do not account for unsaturated hydraulic conductivity,  $K$ , since matric potential is not accounted for which plays a role in unsaturated flow. Matric potential is the capillary rise and surface adsorption forces in soil (how hard the soil holds on to the water) (“Soil Survey Technical Note 6 | NRCS Soils,” n.d.). Thus what is really described is saturated hydraulic conductivity,  $K_s$ , and this is the term that shall be used in this thesis.

Permeability is a term often used interchangeably with either saturated hydraulic conductivity,  $K_s$  or hydraulic conductivity,  $K$  (Chesworth et al., 2021; “Soil Survey Technical Note 6 | NRCS Soils,” n.d.). In this thesis  $K$ ,  $K_s$  and  $k$  shall be used as much as possible to specify what is being described and discussed.

### 1.2.4 Flow regime

Darcy’s equation is based on laminar flow and saturated conditions (Permeability tests, 2019; Sedghi-Asl et al., 2014). In laminar flow the water molecules and streamlines are parallel, water molecules closer to a surface are slowed down due to friction and thus the flow velocity will vary depending on how close to a surface the water is. In turbulent flow the water molecules also move transverse to the overall flow direction. The flow velocity is much more uniform throughout the flow area cross section in turbulent flow (Hölting and Coldewey, 2019).

The Reynolds number,  $Re$ , is a dimensionless parameter that is used to describe the flow behaviour of water in pipes, pores and joints. It is used to determine when flow transitions from laminar to turbulent and its general form is calculated according to (eq 5) (Hölting and Coldewey, 2019).

$$(5) \quad Re = \frac{d \times v \times p}{\eta_{fl}}$$

Where  $d$  = grain diameter (m, mm) (characteristic length for the corresponding current model) ,  $v$  = mean fluid velocity (m/s),  $p$  = fluid density (kg/m<sup>3</sup>) and  $\eta_{fl}$  = dynamic fluid viscosity (Pa x s or kg/s x m) (Hölting and Coldewey, 2019). Dan et al., (2016) found that the relationship between hydraulic gradient and flow velocity is nonlinear in unbound graded aggregate material and can be described by Forchheimers equation.

According to Bear, n.d. there are the following three flow states in porous materials: a) at  $Re$  from 1 to 10, viscous forces are dominant and Darcy’s law is valid. b) at  $Re$  10 to about 100, the flow first transitions from a viscous dominated laminar flow to an inertial dominated laminar flow and then to turbulent flow at the upper end. This flow regime can be called the nonlinear flow regime and Darcy’s law is not valid. c) is for  $Re$  above about 100 and is fully turbulent flow.

### 1.2.5 Forchheimer's equation

Forchheimer's equation is used to describe flow in porous media under transitional or turbulent flow regimes (Dan et al., 2016) and can be expressed according to (eq 6).

$$(6) \quad i = - (a \times v) + (b \times v^2)$$

Where  $i$  = hydraulic gradient,  $a$  and  $b$  are parameters and  $v$  = mean fluid velocity (m/s). Parameter  $a$  accounts for viscous forces, meaning the energy loss that occurs as a result of friction between the fluid and the solid surface. Parameter  $b$  accounts for inertial forces and is solely dependent on the porous medium (Bordier and Zimmer, 2000; Sidiropoulou et al., 2007).

The hydraulic conductivity,  $K$ , can be calculated according to (eq 7), when a non-linear relationship between  $i$  and  $v$  is found, and Forchheimer's equation is fitted to the curve with good agreement.

$$(7) \quad K = \frac{1}{a}$$

Where  $a$  refers to parameter  $a$  in Forchheimer's equation. Or according to (eq 8).

$$(8) \quad K = \frac{p \times g \times k}{\eta_{fl}}$$

Where  $p$  = fluid density (kg/m<sup>3</sup>),  $g$  = gravitational acceleration (m/s<sup>2</sup>),  $k$  = intrinsic permeability (dimensionless) (eq 4) and  $\eta_{fl}$  = dynamic fluid viscosity (Pa x s or kg/s x m) (Dan et al., 2016). There are several different equations for calculating parameter  $a$  detailed by Dan et al., (2016) and parameter  $a$  and  $b$  detailed by Sidiropoulou et al., (2007).

## 1.2.6 Air entrapment

Due to the  $K$  being dependent on the flow of water through the cross sectional area, (eq 3), entrapped air in the soil has a significant impact on measurements. Bouwer (1966) cited in (Chesworth et al., 2021)) states that the pore size and configuration is the controlling factor for  $K$ . Any air stuck in the pores will alter the flow paths available for water and hence reduce  $K$ . Both Lagerlund, (2020) and Sedghi-Asl et al., (2014) use vacuum pumps to get air out of their piezometers before running the test in fixed wall permeameters. A permeameter is a device used to test the  $K$  of a material. Air in the material will decrease the  $K$  (Mohanty et al., 1994; Permeability tests, 2019) and thus if air is present, values produced are not for  $K$ s but for a  $K$ -value with a certain amount of air. Air is also present in the water and de-aired water may be used (Permeability tests, 2019), using de-aired water facilitates reaching complete saturation (Chapuis, 2012).

## 1.3 The primary determining characteristic of hydraulic conductivity

### 1.3.1 Grain size distribution and pore geometry

Bouwer (1966) cited in (Chesworth et al., 2021) states that the pore size and pore geometry is the controlling factor for  $K$ . Dan et al., (2016) found that the passing % by weight of grains < 0.075 mm can be used to control the  $K$ . Hölting and Coldewey, (2019), Statens vattenfallsverk, (1988) and Tennakoon et al., (2012) all state that the fine grained fraction is the controlling factor for  $K$  and that increasing the amount fine grains decreases the  $K$ . An example can be seen in figure 4 where two grain size distribution curves are presented and named according to their comparative  $K$ .

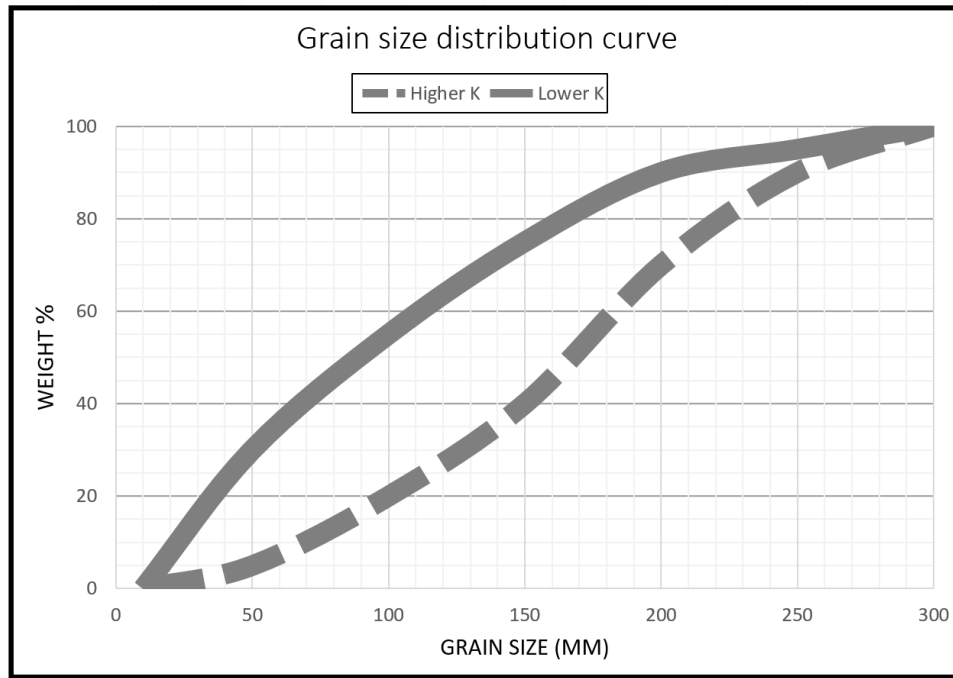


**Figure 4.** Showing two different grain size distribution curves. The dashed line having less fine grained particles will have a higher  $K$  value than the solid line.

Bağcı et al., (2014) conducted fixed wall permeameter tests using 1 or 3 mm steel spheres carefully compacted to ensure a correct porosity based on their uniform shape. The porosity of the 1 mm spheres were 35.01 % and 35.58 % for the 3 mm. At a velocity of 0.05 m/s the pressure drop was five times higher in the 1 mm spheres measured close to the ends of the sample. This is attributed to the smaller pore spaces and more winding flow path in the 1 mm spheres. The irregular pore spaces, mixing of flow paths and separation of microscopic flow fields from the internal geometry are possible causes for flow to transition from laminar to turbulent flow in porous materials (Bağcı et al., 2014).

### 1.3.2 Compaction and particle movement

Dan et al., (2016) tested different mixtures of rock material with the diameter 0 - 5 mm, 5 - 10 mm and 10 - 20 mm in a fixed wall permeameter measuring 100 mm diameter and 450 mm high. They found a linear relationship between compaction and  $K$  above 90% compaction. At the same degree of compaction a higher percentage of finer particles yielded lower  $K$ -values. Statens vattenfallsverk, (1988) state that at higher normal pressure a finer grained material will decrease  $K$  more than a coarser material. If the compaction is higher than the strength of the rock, solid angles can be broken off and more fine particles produced (Chapuis, 2012).

Siddiqua et al., (2011) found that at or near a hydraulic gradient of one, a few or several particles got uplifted by the upwards flow through the fixed wall permeameter. The material tested ranged from 10 - 150 mm in diameter in different gradations. This uplift of particles is concluded to be the reason why data dropped off the trendline for high hydraulic gradients due to this occurring in all tests where particles started moving. Zou et al., (2013) attribute a sharp increase in  $K$ -values in unloaded tests due to local particle movement and call this threshold the critical gradient. Chapuis, (2012) state that internal erosion can be an issue in fixed and flexible wall tests and that if or how much erosion has occurred can be evaluated by analysing the sample in sections for grain size distribution. The tests conducted by Benamar et al., (2019) support this and their tests showed that the overall stability of the sample was not affected by particle movement since only a small fraction of the material is small enough to be transported. However the movement of fine particles reduced the  $K$  and increased the hydraulic gradient where the particles were deposited (Benamar et al., 2019).



### 1.3.3 Flow regime

Dan et al., (2016) found that above a hydraulic gradient of 0.1 the  $Re$  surpassed 10 for almost all of the different mixtures and Forchheimer's equation was used instead of Darcy's law. This was also confirmed by the relationship between hydraulic gradient and flow velocity not being linear. This non linear relationship between hydraulic gradient and flow velocity is the main way of evaluating flow regime in porous materials (Sedghi-Asl et al., 2014). Statens vattenfallsverk, (1988) also states that for coarse grained soils Darcy's law is no longer applicable and the discharge is a square function rather than a linear function of the flow velocity. McCorquodale et al (1978), cited in Hansen, (1992) found that, based on evaluating 1250 column tests, fully turbulent flow occurs at  $Re_{pore} > 500$ . Based on calculating the pore Reynolds number according to (eq 9).

$$(9) \quad Re_{pore} = \frac{V \times m}{\nu \times n}$$

Where  $V$  = bulk velocity (m/s),  $m$  = hydraulic mean radius with no wall effect (m, mm),  $n$  = porosity (dimensionless) and  $\nu$  = kinematic viscosity ( $m^2/s$ ). The hydraulic mean radius is the radius inside the pores that the water flows through and can be calculated according to (eq 10).

$$(10) \quad m = \frac{e}{A_{vs}}$$

Where  $e$  = void ratio (dimensionless) and  $A_{vs}$  = volume specific surface area ( $m^2/kg$ ), which is the surface area of the particles for a specific volume. For example with a  $\nu = 1.003 \times 10^{-6} m^2/s$  and  $n = 0.45$  at a  $m = 1$  mm the minimum velocity to achieve fully turbulent flow occurs at 0.23 m/s (Hansen, 1992). The materials tested by Hansen, (1992) were crushed limestone, graded subrounded gravel and round glass marbles. A hydrostatic head of 2.9 m at the bottom of the fixed wall permeameter was sufficient to produce non-Darcy flow in all materials. Hansen, (1992) also found that depending on how jagged and irregularly shaped the material is, different equations will estimate the non-Darcy flow differently.

Sedghi-Asl et al., (2014) conclude that for rounded materials over 2.8 mm in diameter Darcy's law is not valid. Instead the method to predict the relationship between hydraulic gradient and flow velocity proposed by Sidiropoulou et al., (2007) is the best when compared to several other methods. According to Sedghi-Asl et al., (2014), Sidiropoulou et al., (2007) overestimated the hydraulic gradient for small grains and underestimated for large grains while Ergun (1952), Kovacs (1977) and Ergun-Reichlet methods (1990) cited in Sedghi-Asl et al., (2014) overestimated  $i$  for all grain sizes. Bağcı et al., (2014) found that the permeability of the material varied depending on the flow regime and Leibundgut et al., (2009) stated that groundwater flow turns turbulent  $> 50$  m/d or  $5 \times 10^{-4} m/s$ .

### 1.4 Tracers

A different method to investigate the K or leakage of embankment dams is the use of Tracers. Tracers can be used for many different applications such as tracing phase changes, determining the flowpath and age of water in an aquifer, studying the climate and more. In this section an short overview of tracers will be presented focusing on the relevant information regarding the use of tracers for determining the hydraulic conductivity,  $K$ .

Tracers are divided into two main categories, environmental- and artificial tracers. Environmental tracers include environmental isotopes, hydrochemical substances and pollution tracers. These occur naturally in the water and are added through precipitation and geogenic sources, pollution is not natural to the water but comes from the same input. Artificial tracers include fluorescence-, salt-, radioactive-, activatable-, advanced tracers and drifting particles. Fluorescence tracers are the most commonly used. These are added to the water and are the type of tracer used to determine the  $K$  of a system (Leibundgut et al., 2009).

The properties of an ideal tracer should be distinguishable from the water that is tested, (Dong et al., 2016; Leibundgut et al., 2009) move with the same velocity as the water and not be absorbed by

the materials in the borehole and measuring equipment. Injecting a tracer is a form of contamination and using as little as possible is recommended (Leibundgut et al., 2009). Commonly used artificial tracers have been studied for their human and eco-toxicological effect and several are found to be harmless, for example uranine, eosin yellow, amidorhodamine G (Behrens et al., 2001). Long term metabolism of fluorescent tracers needs to be taken into account. The general approach when using tracers is to measure a known volume or concentration of a tracer over time and space. Using a combination of different tracers especially combining artificial- with environmental tracers, reduces the error potentially caused by either tracer method (Leibundgut et al., 2009).

## 1.5 Research questions

Coarse grained soil materials are used when building embankment dams. Understanding the behaviour of these materials is a key parameter for designing safe and long lasting embankment dams. This thesis aims to fill a knowledge gap regarding hydraulic conductivity measurements in coarse grained materials by answering the following questions:

- What are the state-of-the-art methods used to derive hydraulic conductivity from porous materials, in the laboratory and in the field?
- What methods are suitable for coarse grained materials?
- What are the controlling characteristics for hydraulic conductivity?

## 2. Method

A literature survey was conducted using databases and keywords listed in table 1. All sources were checked against Cabells predatory reports list and peer-reviewed sources were used as much as possible. In total over 160 books, articles and online contents from the fields of dam construction, road building, soil science, railway industry and more, were reviewed.

**Table 1.** Showing databases used and examples of keywords used.

Databases	Examples of keywords
Uppsala university library search engine	Hydraulic conductivity AND coarse grained OR train tracks OR rockfill OR support rockfill OR embankment dams OR ...
DIVA	Permeability AND drainage bed OR measurement OR method OR ...
SIG-line	Hydraulisk konduktivitetmätning
USGS	Permeabilitetsmätning
Energiforsk	Mätmetoder för hydraulisk konduktivitet
SKB	Pump test OR celltryckspermeameter OR falling head test OR ...
ResearchGate	Hydraulic conductivity controlling characteristics
Engineering Village	Turbulence in coarse grained materials
Scopus	Embankment dams
Google scholar	Reynolds numbers
Google	Tracer AND hydraulic conductivity

## 2.1 Demarcation

This thesis presents an overview and not a detailed study on every measurement method. Therefore examples of equations are given when needed, and not all possible equations or their drawbacks and advantages. Falling- / constant- / rising head has neither been elaborated on and only mentioned as a possibility. Air entrapment is only mentioned and not elaborated on in this thesis. Parameters  $a$  and  $b$  from Forchheimer's equation are not elaborated on.

## 3. Results

### 3.1 Laboratory methods

#### 3.1.1 Fixed wall permeameter

A fixed/rigid wall cylindrical permeameter or “rörpermeameter” is the most common laboratory test method for coarse grained materials (David Suits et al., 2005; Koohmishi and Palassi, 2018; Luo et al., 2020; Permeability tests, 2019) or materials with a saturated hydraulic conductivity,  $K_s > 1 \times 10^{-5}$  m/s (D18 Committee, n.d., n.d.). The basic setup is a rigid cylinder where the test sample is placed between two porous discs, with a high enough  $K_s$  so as not to affect the measurements. Before measurements begin the air needs to be removed from the testing material, this can be done using vacuum pumps (Chapuis, 2012; Lagerlund, 2020; Sedghi-Asl et al., 2014).

A common setup for a constant head test is using an adjustable overhead tank, where the water level in the overhead tank is kept constant throughout the testing procedure, figure 5 (Permeability tests, 2019; Tennakoon et al., 2012). Other setups include the falling head test, constant tail test and raising tail test further described in (Permeability tests, 2019). One way to measure the volume of water passing through the sample is to collect it and weigh it, figure 5 (Koohmishi and Palassi, 2018; Permeability tests, 2019).

Permeability tests, (2019) recommends measuring the elevation heads at glands placed along the sample within the porous discs as to reduce inaccuracies from head losses in tubes, valves and filter discs. Lagerlund, (2021) states that this is due to the large pores in coarse grained materials. If the pore structure in the material is larger than the tubes, valves and filter discs these will be the determining factor for the  $K_s$ . The minimum internal diameter of the permeameter should be 4 - 10 times  $d_{\text{max}}$  (ASTM 2011a cited in Chapuis, 2012; ASTM 2006 cited in Ferdos et al., 2015). This is to reduce seepage along the wall of the testing cylinder. Permeability tests, (2019) state that a hydrophobic coating can be used to reduce wall-seepage further. According to Lagerlund, (2021) there is no need for a hydrophobic coating in coarser materials, and due to the large pores within a sample of this size this is no longer needed. To check if the flow is primarily in large pores or along the wall a non-reactive tracer test can be utilized (Chapuis, 2012). AS 1289.6.7.3-1999 cited in Tennakoon et al., (2012) states a minimum sample height of five times  $d_{\text{max}}$  and (Permeability tests, 2019) states a minimum internal height to be six times  $d_{\text{max}}$ .

Materials tested in different permeameters varied from coarse rockfill  $d = 10 - 150$  mm (Siddiqua et al., 2011), coarse soil  $d = 0 - 50$  mm with  $K_s = 0.1 - 5 \times 10^{-4}$  m/s (Benamar et al., 2019) and railway ballast with different kinds and degrees of fouling with  $K_s = 1 - 4.7 \times 10^{-5}$  m/s (Paiva et al., 2015; Tennakoon et al., 2012).

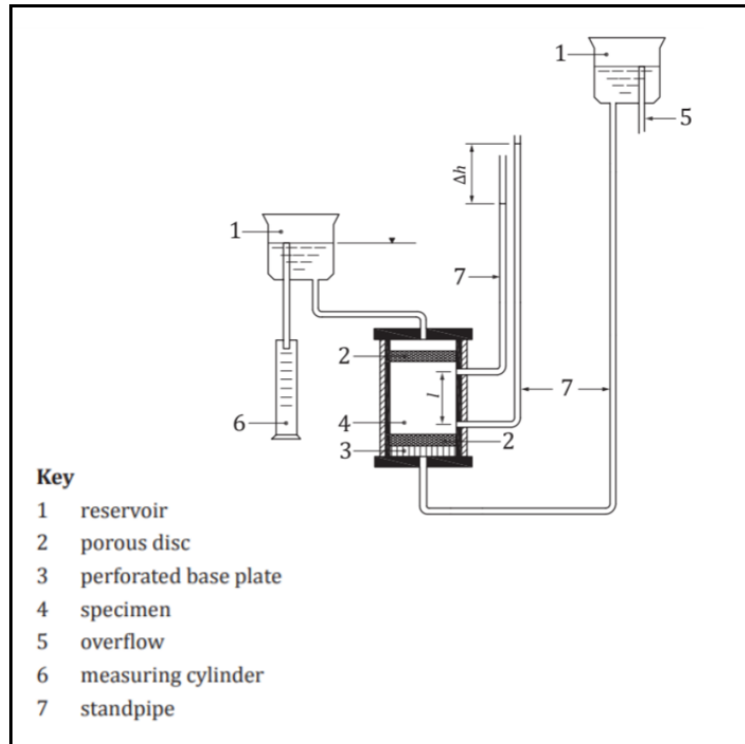


**Figure 5.** An example of fixed wall permeameter (*Permeability tests*, 2019).

An example of a large fixed wall permeameter is the one used by Lagerlund, (2020). It has an internal diameter of 1000 mm, a maximum sample height of 1100 mm and can accommodate grain sizes up to 250 mm. The filter zones are constructed out of a 300 mm thick golf ball layer, a 30 mm steel plate with holes in it and a fine steel mesh closest to the sample. This is in order to distribute the water evenly across the entire sample width. During testing the hydraulic gradient is controlled through a fixed height reservoir and an adjustable outlet height. The water flows vertically up through the sample or down depending on the configuration. The elevation head is measured by 16 glands along the sample height distributed across 4 levels (Lagerlund, 2020).

### 3.1.2 Flexible wall permeameter

A flexible wall permeameter / triaxial permeameter or “celltryckspermeameter” is a laboratory method used when tests are performed on a pressurized sample. The test can be conducted in a triaxial device with porous discs sealing the sample from the bottom and the top and a water measuring device, for example collecting the water and measuring it, figure 6 (*Permeability tests*, 2019).

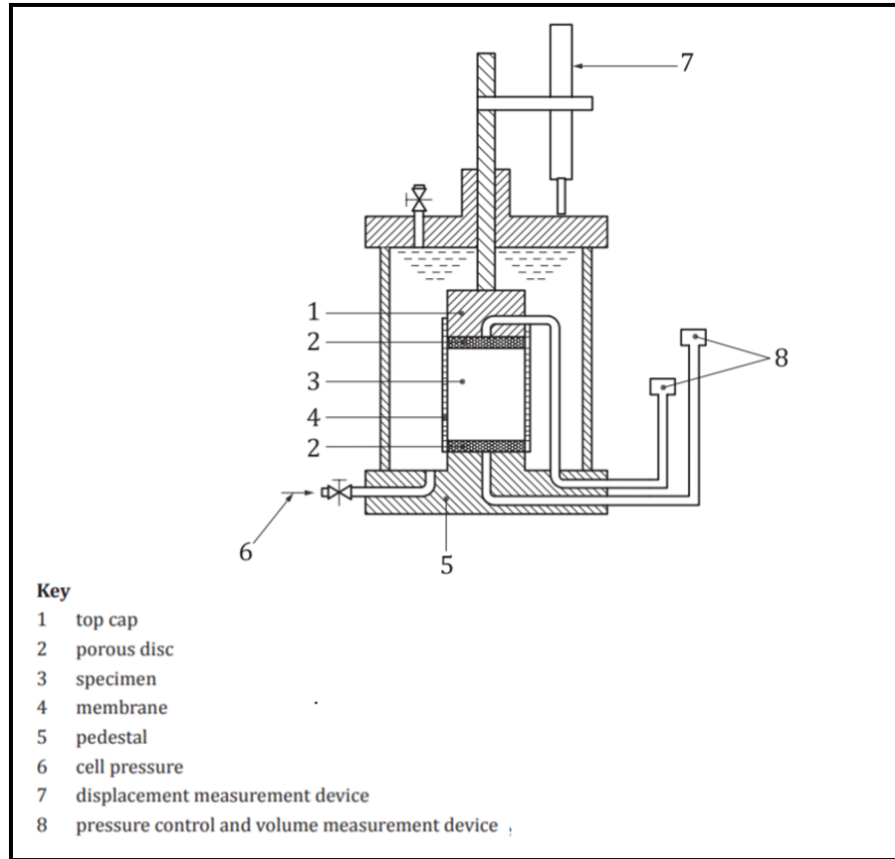


**Figure 6.** An example of a flexible wall permeameter (*Permeability tests*, 2019)

Materials tested were residual soil, with  $K_s = 9.48 \times 10^{-7} - 6.25 \times 10^{-10}$  m/s (Samingan et al., 2003), kaolinite and marine clay with  $K_s = 8 \times 10^{-11} - 2 \times 10^{-9}$  m/s (Sridhar and Robinson, 2013), well-graded sandy-silt soil with  $K_s = 4 \times 10^{-9} - 10^{-8}$  m/s (Kandalai et al., 2018) and fine-grained soils with  $K_s = 7.8 \times 10^{-9} - 10^{-8}$  m/s (Benson and Yesiller, 2016). No device described by Samingan et al., (2003) could measure  $K_s > 10^{-5}$  m/s. D18 Committee, n.d. state that for a  $K_s > 1 \times 10^{-5}$  m/s method D2434 (fixed wall permeameter) should be used. According to Daniel et al., (1985) flexible wall permeameters are better than fixed wall permeameters at reducing side wall leakage as well as testing samples under effective stress.

### 3.1.3 Plane-strain permeameter

A plane-strain permeameter is designed to test soil samples under horizontal and vertical load. It consists of a square sample chamber where one side wall and one porous plate are mounted to soft rubber in order to move. One wall moves as the vertical pressure cylinders push on it. Another horizontal pressure cylinder is mounted in order to control the horizontal pressure, figure 7 (Zou et al., 2013).

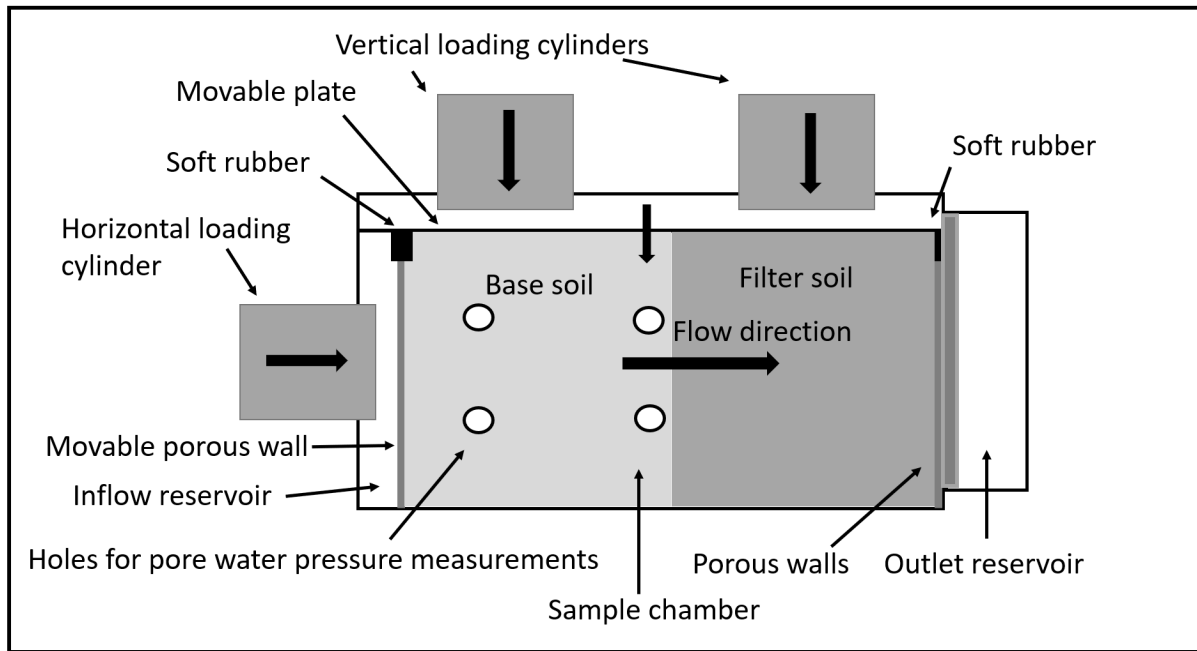


**Figure 7.** A simplified figure of a plane-strain permeameter. The pressure cylinders apply pressure to the sample through the movable plate and movable porous wall, which compresses the soft rubber. The porous walls allow water to flow through during testing and pore water pressure measurements taken through holes in the sample chamber (adapted from Zou et al., 2013).

A water reservoir with a float to maintain a constant water level is used to adjust the water pressure. Inlet water pressure sensor, pore pressure sensor, pressure gauges in the cylinders and a piston stroke dial are used to collect data. It could accommodate soil samples roughly 800 x 400 x 400 mm and a maximum grain size of 80 mm. The movable plate and the movable porous wall allow the chamber to vary from 400 - 460 mm in height and 740 - 860 mm in length. The maximum vertical pressure was 2000 kN and 1000 kN in the horizontal direction. The maximum water pressure was 3 MPa with a maximum discharge of 117 cm<sup>3</sup>/s (Zou et al., 2013).

Materials tested by Zou et al., (2013) came from the core soil (gravelly clay) and granular filter of the Shuangjiangkou Dam. Tests were conducted with both a core sample and a filter sample in the testing chamber to simulate the transition from filter to core in the dam. The core soil had a grain size from 0.07 - 100 mm and thus any grains larger than 60 mm were replaced with an equal amount of grains ranging from 5 - 60 mm, due to the maximum grain size of the permeameter being 80 mm. The granular filter had a grain size from 0.004 - 20 mm. Three tests were conducted with the same material and testing parameters in order to ensure repeatability from the testing method. The materials had a  $K_s$ -value of  $4 \times 10^{-8}$  -  $10^{-7}$  m/s depending on the volumetric strain. Tests were conducted with no loading of the specimen, one directional compression and two directional compression. The results showed that the  $K_s$  decreased and the critical gradient for particle movement increased under higher volumetric strain (Zou et al., 2013).

#### 3.1.4 Evaporation method

The evaporation method by Schindler (1980) cited in Hartmann et al., (2020) and Peters and Durner, (2008), is a laboratory method used to determine the water retention and hydraulic properties of a soil sample. During testing a saturated sample is dried evenly at a slow rate through evaporation. The matric potential is measured at two heights within the sample by tensiometers and the weight of the sample is continuously measured. The water retention curve is calculated based on the matric potential and soil water content. The hydraulic gradient can be calculated from the matric potential and flow rate from decrease in water content. Hydraulic gradient and flow rate are then used to calculate  $K$  (Hartmann et al., 2020; Peters and Durner, 2008). Samples measured by Hartmann et al., (2020) were different moraine samples that measured 250 cm<sup>3</sup> and sandy loam soil and clay with a

sample height of 6 cm was used by Peters and Durner, (2008). Masaoka and Kosugi, (2018) developed an “improved evaporation method” that was estimated to be able to measure  $K$  up to roughly  $3 \times 10^{-6}$  m/s (27 cm/day).

### 3.1.5 Multistep outflow permeameter

The multistep outflow permeameter is a laboratory method used to determine soil water retention and hydraulic properties (Bagarello et al., 2000). The test can be performed on disturbed or undisturbed soil samples. First the sample is saturated and then placed in a modified Tempe pressure cell, figure 8, measuring 8.25 cm in outside diameter and 6 cm long (Tuli et al., 2001) on top of a porous plate (Bagarello et al., 2000). Tensiometers are used to measure the matric potential. The water level in the sample is then lowered in increments and the outflow water is collected and measured. The experiment generates outflow vs. time and pressure head vs. time measurements that then can be analyzed and  $K$  calculated (Bagarello et al., 2000; Tuli et al., 2001).

Materials measured had a  $K$  of around  $3 \times 10^{-6}$  m/s (0.01918 cm/min) (Tuli et al., 2001) and  $5 \times 10^{-6}$  -  $3 \times 10^{-5}$  m/s (20-100 mm/h) in sandy loam soil with a relatively high sand and gravel content (Bagarello et al., 2000). For coarse materials an error due to the fitted retention function can become significant, and thus provide unreliable data (Peters and Durner, 2006).

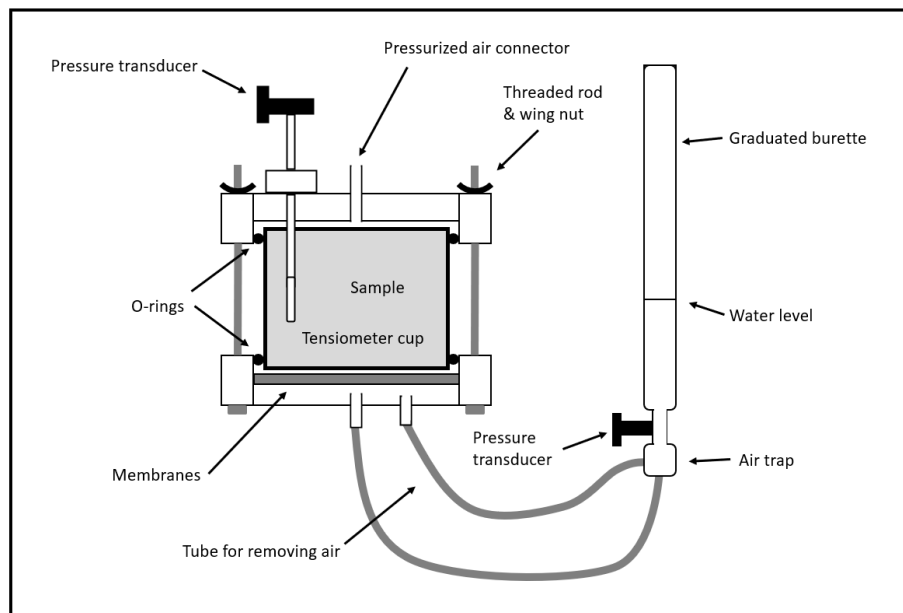


**Figure 8.** A simplified figure of a modified tempe pressure cell used as a multistep outflow permeameter (adapted from Tuli et al., 2001).

## 3.2 Field methods

### 3.2.1 Guelph- / well- / borehole permeameter (GP)

The Guelph- / well- / borehole permeameter or shallow well pump-in method, referred to as GP in this thesis, is a field method to determine  $K$ , sorptivity and the matric flux potential (Angulo-Jaramillo et al., 2016). To conduct a measurement a vertical hole is dug. The dimensions vary depending on the soil type. According to Reynolds and Elrick (2005) cited in Angulo-Jaramillo et al., (2016), the most common wells are 0.1 - 1 m deep and 0.04 - 0.1 m in diameter. The walls of the hole must not be smeared from the digging procedure or action to remedy this must be taken. The permeameter consists of a support tube with outlets that is placed on the bottom of the well. To this tube a reservoir is attached with a control system, to ensure a constant water level in the well. The outflow from the support tube is designed to limit flow velocity in order not to damage the walls of the well, figure 9.

When conducting a measurement the well is filled to the desired level and the time between two water levels in the reservoir is measured. When a steady state for the infiltration has commenced measurements are taken. A steady state is achieved when the saturated area created by the water in the

well stops expanding. By knowing the amount of water that has drained into the well of known dimensions, the  $K$  value can be calculated (Angulo-Jaramillo et al., 2016; Reynolds and Elrick, 1986). The compilation of 10 studies done with the GP compared to other methods done by Angulo-Jaramillo et al., (2016), show that no materials coarser than sand were measured. The range of which a commercially available GP can measure  $K = 10^{-8} - 10^{-4}$  m/s according to Angulo-Jaramillo et al., (2016).

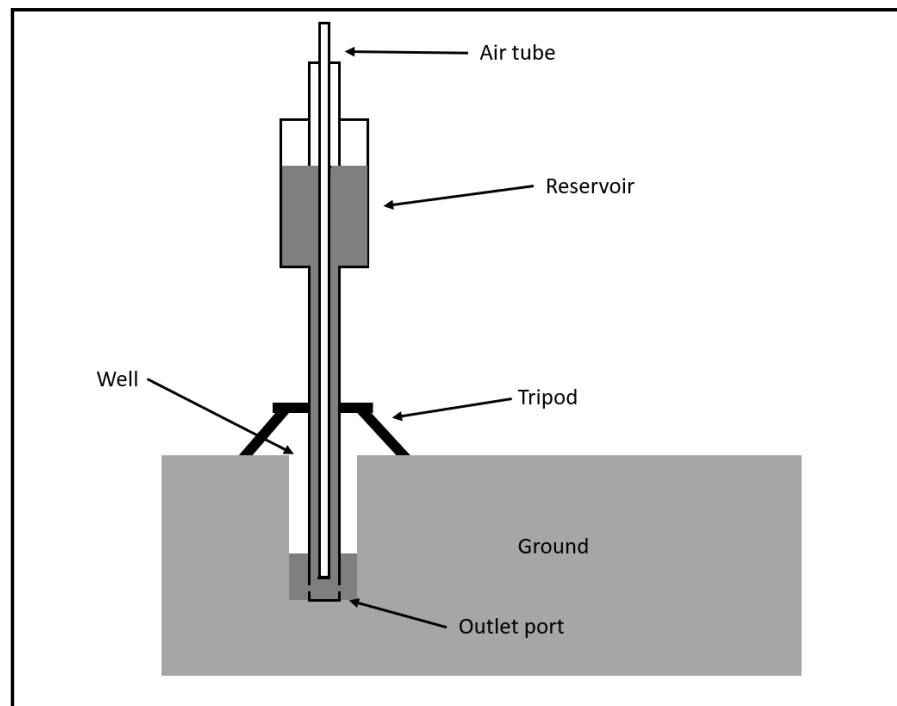


**Figure 9.** A simplified figure of a Guelph- / well- / borehole permeameter (GP) (adapted from Reynolds and Elrick, 1986).

### 3.2.2 Drive point method

The drive point method is based on the Guelph permeameter (GP) but uses a drive point instead of a dug/augured well, figure 10. The drive point can be pushed, rotated or vibrated into the ground. The outflow tube from the GP control system and reservoir is connected to the drive point casing. The water level in the drive point is kept at or below the height of the outflow screen. During testing the water level is kept constant and after a steady state has been achieved the testing begins. The time between two levels in the reservoir are measured. By knowing the amount of water that has drained into the ground, the height of the water in the drive point and the radius of the outflow screen the  $K$ s value can be calculated.

Materials measured were well sorted medium-coarse sand and had a  $K$  value of around  $3 \times 10^{-4}$  m/s (Reynolds and Lewis, 2012). Due to the outflow screen only directing water radially and the conical tip being solid, no vertical flow of water occurs in the GP method. Therefore the GP calculations are modified to account solely for horizontal flow (Angulo-Jaramillo et al., 2016; Reynolds and Lewis, 2012). Reynolds and Lewis, (2012) found that the drive point method produced similar results to pump and slug tests in coarse sand. They also found the drive point method to be inaccurate in soils that deteriorate structurally when wetted due to the soil collapsing around the drive point.



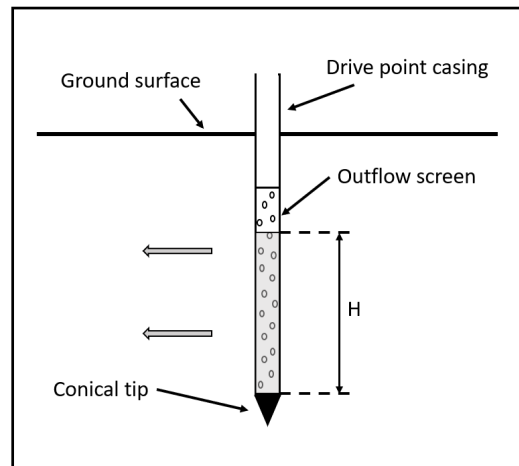


**Figure 10.** Displaying a drive point inserted into the ground. The height of the water inside the drive point ( $H$ ) must not exceed that of the outflow screen. The conical tip is of the same width as the drive point casing. The arrows represent the radial flow of water (adapted from Reynolds and Lewis, 2012).

### 3.2.3 Pump- / borehole method

The pump- / borehole method is based on measuring the in- or outflow of water from a borehole of known dimensions. Water permeability tests in a borehole using open systems, (2012) recommend using the following tests for soils with a  $K > 10^{-6}$  m/s; a constant flow rate test, either drawing water from the borehole, if it goes deeper than the groundwater surface, or by supplying a constant flow into the borehole (Hölting and Coldewey, 2019). For soils with a  $K$  value ranging from  $10^{-6}$  m/s to  $10^{-9}$  m/s a variable head is recommended. This is done by generating an immediate change in hydraulic head in the borehole and measuring the change in hydraulic head over time. A constant head test is recommended for soils with a  $K$ -value ranging from  $10^{-4}$  -  $10^{-7}$  m/s. Here a constant head is maintained in the desired section of the borehole and the flow rate is measured over time.

The equipment needed is a drill, casing, piezometer, water reservoir/supply system, bail or pump system, constant flow device, filter material and/or perforated tube, in borehole/casing water level measurement device, time recorder and a setup to determine the flow rate for the constant head or constant flow tests. Depending on what test is conducted not all of the equipment is needed, figure 11 and 12 (Water permeability tests in a borehole using open systems, 2012).

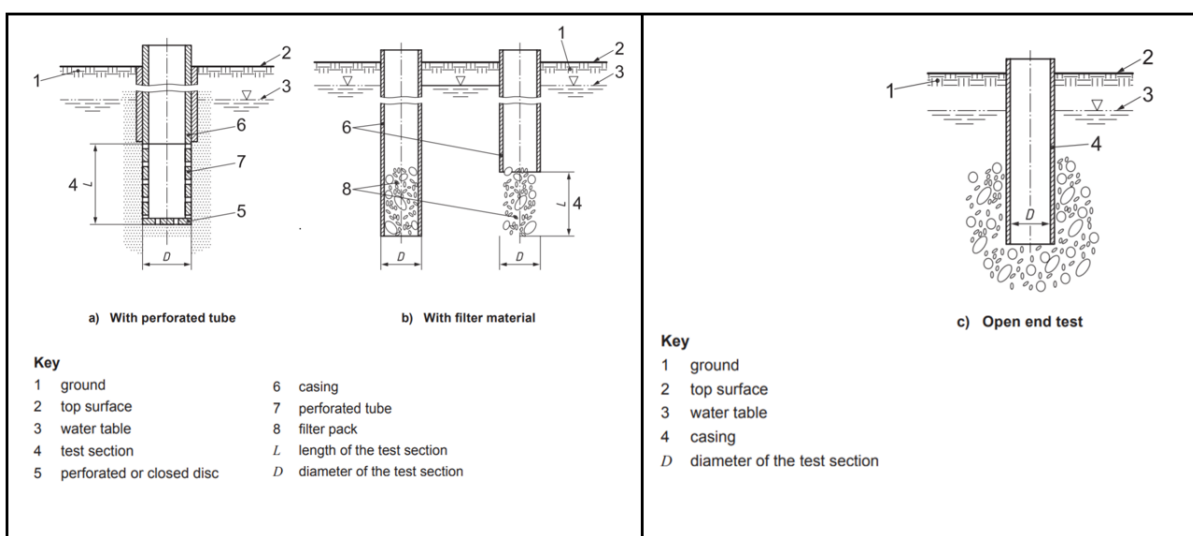


**Figure 11.** Different setups for the borehole- / pump method in unstable rock. **a)** uses a perforated tube that is inserted before the casing is withdrawn, **b)** uses a filter pack and the casing is withdrawn **c)** is an open end test where water only flows out of the bottom of the borehole, (modified from *Water permeability tests in a borehole using open systems*, 2012).

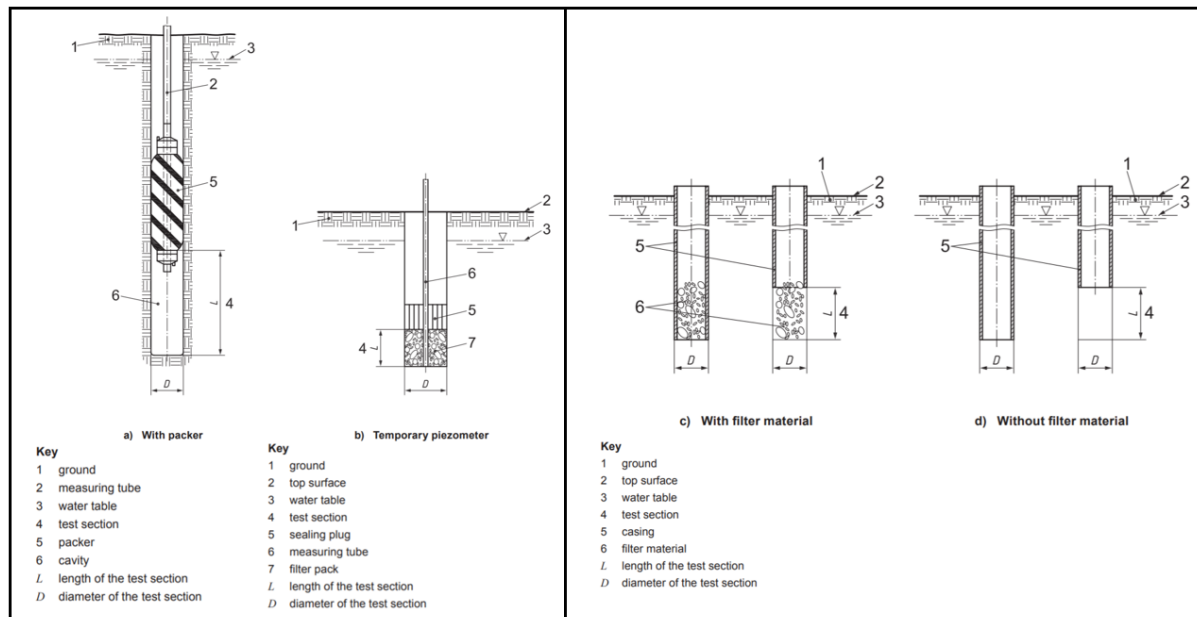


**Figure 12.** Different setups for the borehole- / pump method in stable rock. **a)** uses a packer to seal the borehole, **b)** is called a temporary piezometer where a measuring tube is inserted into a filter pack and the borehole is sealed with a plug. **c)** and **d)** are with or without filter material, in both cases the casing is withdrawn, (modified from *Water permeability tests in a borehole using open systems*, 2012).

Constant head and free infiltration tests were conducted by (Ferdos et al., 2015), in coarse rockfill material. The material had grains varying from 0 - 1000 mm in diameter. The characteristic/representative grain size was 128 mm in diameter. The data was analyzed both assuming laminar flow as well as turbulent flow nearest to the borehole and used a two-regime flow analysis. It was found that the flow was transitional rather than fully turbulent and the  $K$  calculated using Darcy's law and laminar flow matched the measured data the best. The material had a  $K$ -value of 0.10 m/s (Ferdos et al., 2015).

Tests can be carried out in both saturated and unsaturated soil. Coarser soils are usually unsaturated due to the high  $K$  value and the flow pattern from the well will differ from saturated tests, figure 13 (*Water permeability tests in a borehole using open systems*, 2012). Hölting and Coldewey, (2019) remark that results gained from pumping tests are generally a rough estimate due to the circumstances of the test; layer thickness varies in the ground, erosion can occur and the grain size distribution varies.

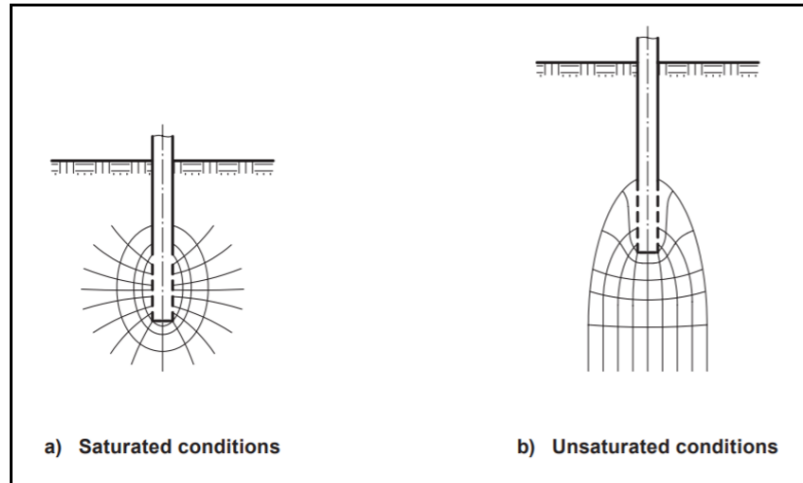


**Figure 13.** Showing a simplified view of how the flow pattern from a well into unsaturated vs saturated soil differs (modified from (*Water permeability tests in a borehole using open systems*, 2012).

### 3.2.4 Single well technique / point dilution method

Single well / borehole technique or point dilution method uses a single borehole or well where a tracer is added and the dilution of the tracer is measured over time (Dong et al., 2016; Leibundgut et al., 2009). The  $K$  can be calculated using Darcy's law by knowing the hydraulic gradient and filter velocity which is calculated from the dilution logs (Leibundgut et al., 2009).

After drilling the well a filter pipe should be installed with a high enough  $K$  as not to disturb the water flow. The direction of the water flow can be measured either using a direction sensitive detection device (Leibundgut et al., 2009) or the average vertical and horizontal flow can be determined by moving the detection device up and down in the borehole until two complete concentration curves have been established, figure 14. This requires the tracer to be released at a certain height in the borehole (Dong et al., 2016).

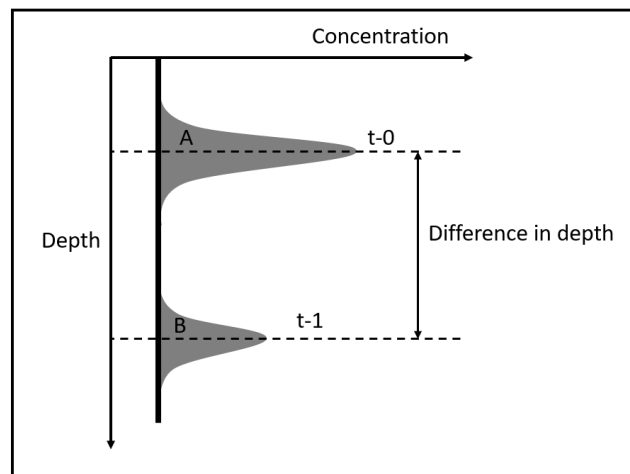


**Figure 14.** Showing two complete dilution curves distinct from the background concentration. Depth, concentration and time is measured (adapted from Dong et al., 2016).

According to Dong et al., (2016) and Leibundgut et al., (2009) flow velocities over  $5 \times 10^{-7}$  m/s can be measured. Below  $5 \times 10^{-7}$  m/s the diffusion of the tracer becomes too significant. Up to  $5 \times 10^{-4}$  m/s Darcy's law can be used to calculate  $K$ , but above that the groundwater flow becomes turbulent and other calculations are required (Leibundgut et al., 2009). Flow velocities measured by Jamin et al., (2020) and Maldaner et al., (2018) ranged from  $10^{-5}$  - 0.1 m/s and were recorded in sand and dolostone bedrock.

### 3.2.5 Quantitative determination of hydraulic conductivity using tracers

By releasing a certain amount of tracer in one location and measuring the concentration at a known distance away from that point, figure 15 an estimate for the  $K$  can be determined (Leibundgut et al., 2009). The release point can be a well, a borehole, a spring or any other location where the tracer can be released (Bodeving, 2020; Hölting and Coldewey, 2019; Leibundgut et al., 2009). In order to calculate  $K$  correctly the boundary conditions are included. Depending on the setting, the water can flow in one, two or three directions, figure 15, this will affect the measurements (Bodeving, 2020; Leibundgut et al., 2009).

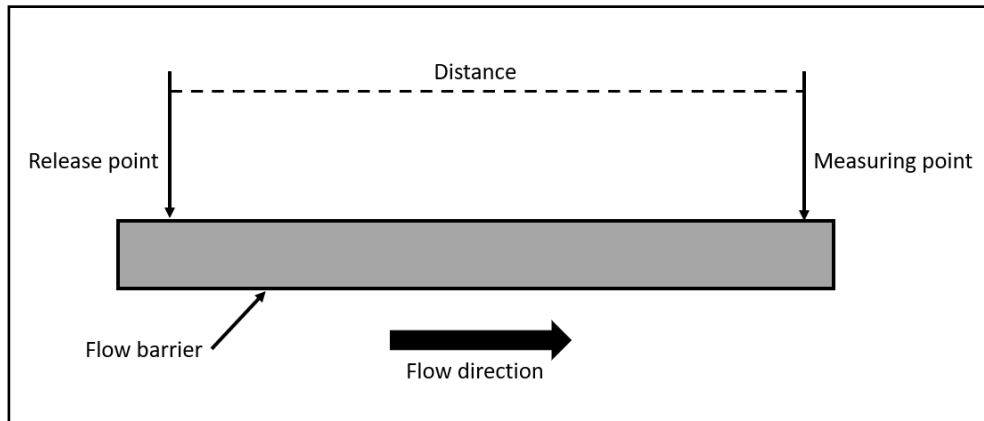


**Figure 15.** A test setup for a tracer test with the release point and measuring point at a known distance and a known flow barrier (adapted from Bodeving, 2020).

During testing the tracer is released in a single pulse or as a constant injection. In both cases the exact concentration and quantity of tracer have to be known (Leibundgut et al., 2009). The concentration of the tracer is measured over time at the measuring point. The concentration over time is recorded in a breakthrough- / transit curve, figure 16 (Bodeving, 2020; Hölting and Coldewey, 2019) and the discharge can be calculated using the trapezoidal approach as well as mass recovery of the tracer (Leibundgut et al., 2009). Average flow velocity is calculated by knowing the boundary conditions and hence the area water flows through (Leibundgut et al., 2009). The  $K$  can be calculated by knowing the difference in hydraulic head between injection - and measuring point, the average flow velocity and the porosity. Materials measured were unconsolidated weathered rock and had an average flow velocity of 0.011 and 0.045 m/s (Bodeving, 2020). This method has also been used to detect leakage pathways in dams (Dong et al., 2016).

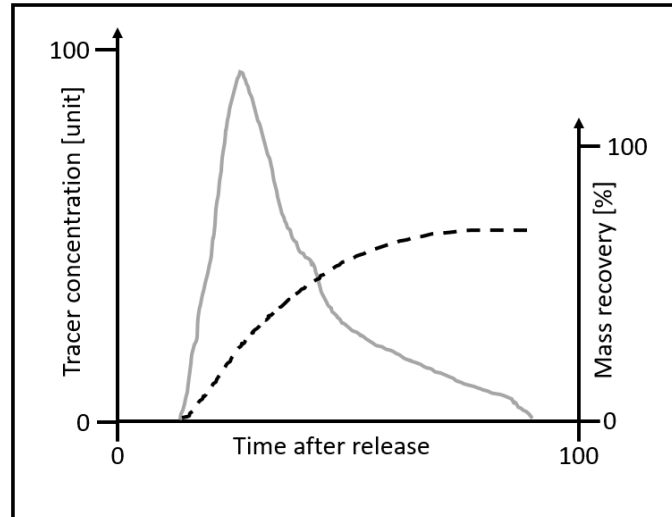


**Figure 16.** A breakthrough- / transit curve where the solid grey line is the tracer concentration and the dotted black line the mass recovery (adapted from Bodeving, 2020).

### 3.2.6 Disc permeameter / Tension infiltrometer

A disc permeameter, also called a tension infiltrometer in the US, is a field infiltration measurement device. It applies a constant negative potential (tension) to the soil in order to avoid macropore (large pores) flow. In order to favor soil matrix flow, which is the dominant flow during infiltration from rainfall and irrigation. The permeameter consists of a 20 - 25 cm cylinder pushed into the ground at the measuring location. Sand is then placed within the cylinder to provide a smooth contact surface and avoid surface soil disturbance during testing. To this cylinder is a plate with a water reservoir and bubbling tower connected, that generates the negative potential ranging from -200 mm - 0 mm, figure 17 (Perrouc & White 1988 cited in Ankeny et al., 1991; Bagarello et al., 2000; Eusufzai and Fujii, 2012; Joel and Messing, 2000; Mohanty et al., 1994).

$K$  is calculated based on steady-state flow and the device can be set-up to measure unsaturated  $K$ ,  $K$  at near saturation and  $K_s$ . Materials measured were volcanic ash soil with Andisol and clay loam texture, sandy clay with a clay content of roughly 30% and sandy loam soil. The  $K_s$  values varied from  $5.7 \times 10^{-9}$  -  $1.9 \times 10^{-5}$  m/s (Bagarello et al., 2000; Eusufzai and Fujii, 2012; Joel and Messing, 2000; Mohanty et al., 1994). A disc permeameter is limited to measuring soils with a lower  $K$  value than that of the conductance material, typically sand, and the porous membrane of the permeameter (Mohanty, Kanwar & Everts 1994).

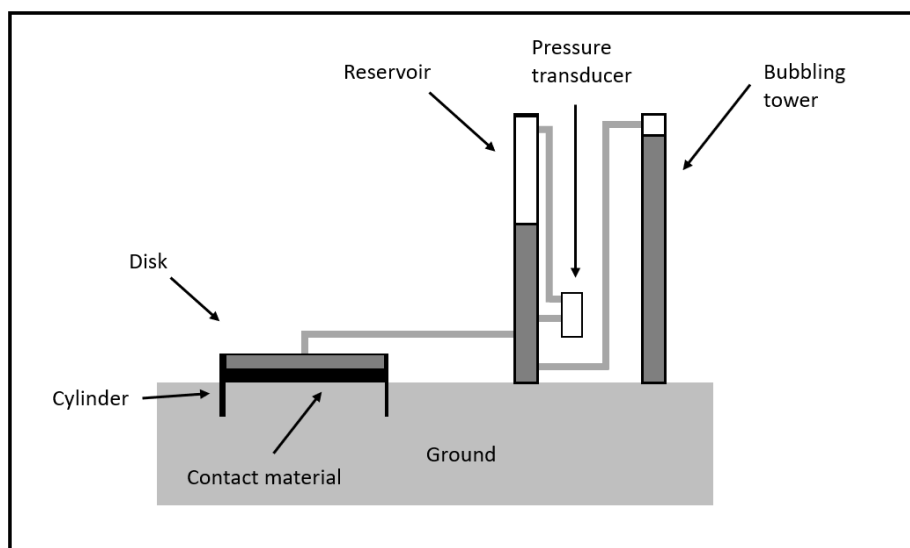


**Figure 17.** A simplified figure of a disc permeameter / tension infiltrometer (adapted from Castiglione et al., 2005).

### 3.2.7 Velocity- / falling head permeameter

The velocity- / falling head permeameter is a field method where the infiltration rate of the soil is used to calculate  $K_s$ . It was modified for field use by Merva (1987) cited in Mohanty et al., (1994). Measurements are conducted using a 8.4 cm diameter cylinder with a closed cap that is pushed into the ground about 7 cm. Two hoses are connected to the cap, one to let air out and one connected to a water tank as well as an observation tube. The soil core within the cylinder is then saturated and the time it takes the wetting front to move through the soil core is recorded using the observation tube.

The  $K_s$  is then calculated using the diameter and length of the cylinder and the time it took the wetting front to exit the soil core. Soils measured where glacial-till soil had a  $K_s$  value ranging from  $7.1 \times 10^{-8}$  -  $3.46 \times 10^{-5}$  m/s ( $7.1 \times 10^{-5}$  -  $3.46 \times 10^{-2}$  mm/s) (Mohanty et al., 1994).

## 4. Discussion

Several different methods for measuring hydraulic conductivity,  $K$ , and saturated hydraulic conductivity,  $K_s$ , have been presented, not all are suitable for coarse grained materials found in embankment dams. Table 2 summarizes all the methods found and rates them according to suitability for coarse grained materials. Methods found suitable are discussed in this chapter, divided into laboratory- and field methods. The topics presented in section 1.3 “The primary determining ...” are not discussed separately for each method, since most of these can have an effect on several if not all methods, but are discussed in their own section.

The discussion is written based around embankment dams and the implications these measurements might have on the construction, monitoring and maintenance of these dams.

**Table 2.** Compilation of all measurement methods presented in the results, organized according to laboratory- / field method, materials measured in the studies used in the results,  $K/K_s$ -values in those materials, my own assessment regarding suitability for coarse grained materials and an explanation to that assessment.

Method	Laboratory / Field	Materials measured	$K$ -values of materials measured (m/s)	Suitable for coarse grained materials?	Explanation
Fixed wall permeameter	Laboratory	Coarse rockfill, coarse soil, railway ballast with different kinds and degrees of fouling	$1E-7 - 1$	<b>Yes</b>	Easily scalable to accommodate large grain sizes
Plane-strain permeameter	Laboratory	Core soil and granular filter from an embankment dam	$4E-8 - 1E-7$	<b>Yes</b>	Scalable to accommodate large grain sizes
Flexible wall permeameter	Laboratory	Residual soil, kaolinite clay, marine clay, well-graded sandy-silt soil and fine-grained soils	$8E-11 - 9E-7$	<b>No</b>	No need to seal the edges in coarser materials
Evaporation method	Laboratory	Moraine, sandy loam soil and clay	$> 3E-6$	<b>No</b>	Small sample size, coarse materials having a very low matric potential
Multistep outflow permeameter	Laboratory	Sandy loam soil with a relatively high sand and gravel content	$3E-6 - 3E-5$	<b>No</b>	Error in fitted retention function for coarse materials
Drive point method	Field	Well sorted medium-coarse sand	$\approx 3,00E-04$	<b>Yes</b>	Only limited by the wetted stability of the material and the ability to insert the drive point
Pump- / borehole method	Field	Coarse rockfill	$1E-7 - 1E-1$	<b>Yes</b>	Several different setups available depending on the material characteristic
Single well technique / point dilution method	Field	Sand and dolostone bedrock	$1E-5 - 1E-1$ (flow velocity, not $K$ )	<b>Yes</b>	No upper limit for flow velocity
Quantitative determination of $K$ using tracers	Field	Unconsolidated weathered rock	$1.1E-2 - 4.5E-2$ (flow velocity, not $K$ )	<b>Yes</b>	No upper limit for flow velocity
Disc permeameter / tension infiltrometer	Field	Volcanic ash, sandy clay and sandy loam soil	$6E-9 - 2E-5$	<b>No</b>	Limited by the contact material, typically sand
Velocity- / falling head permeameter	Field	Glacial-till soil	$7E-8 - 3E-5$	<b>No</b>	Inability to push the small cylinder into the ground
Guelph- / well- / borehole permeameter	Field	Finer materials than sand	$1E-8 - 1E-4$	<b>No</b>	Inability to dig a well in coarse material of such small sizes

#### 4.1 Laboratory methods suitable for coarse grained materials

The material tested in the laboratory will have to be extracted from the dam or tested before the dam is built. If the grain size distribution for the dam is known and/or the material used for the dam is available, this can also be used to test the  $K$  of the dam. However in all of these cases, since material is compacted in a dam by different methods from the laboratory, a laboratory sample will never be fully representative of the actual conditions in the dam.

##### 4.1.1 Fixed wall permeameter

If a hydrophobic coating is used to reduce sidewall leakage (Permeability tests, 2019) in a more fine grained sample, would this then affect the cross sectional area that is used to calculate  $K$  if Darcy's

law is used? If samples are tested and particle movement (Siddiqua et al., 2011) or uplift of the entire sample becomes a problem (only when the flow runs from the bottom up), A system to apply pressure on the top porous disc could be used. This system could be constructed out of springs that are compressed, rubber with the same function or hydraulics for more control. This could not only serve to keep the sample in place but also add a certain degree of compression to the sample.

The fixed wall permeameter is the most commonly found laboratory method for coarse grained material. This is likely due to its simple design and hence cost effectiveness. However if more measurements conclude, as found by Zou et al., (2013) that  $K$  decreases and the critical gradient increases under compressive strain, it can be argued that these properties make a dam safer and hence more of these tests would be beneficial to gain a better understanding of how compressive strain affects  $K$ .

#### 4.1.2 Plane-strain permeameter

Zou et al., (2013) was the only source found using a plane-strain permeameter or a device similar in function for testing coarse grained materials. The effect volumetric strain had on  $K$  and critical gradients indicate that a certain base material can not be expected to behave the same at various depths in a dam. An argument can be made that if a material is to be used under high volumetric strain, such as within an embankment dam, that material should be tested under those compressive forces to evaluate its hydraulic properties for said application. An increase in critical gradient is positive for an embankment dam and thus implications for construction would likely be none or minimal.

This outcome could be the reason these permeameters are not more common. The well known effect compaction has on  $K$  and compaction practice in constructing embankment dams (Statens vattenfallsverk, 1988) means that dams are safer under higher volumetric strains.

### 4.2 Field methods suitable for coarse grained materials

#### 4.2.1 Drive point method

The drive point method is useful in that it can be applied anywhere on the reachable surface on the dam with very little to none damage to the dam itself. However, if it can reach deep enough to provide useful information in the field is questionable in coarse rockfill dams. In more uniformly graded dams this method could be more suitable and possibly used as a tracer dispersion technique.

#### 4.2.2 Pump- / borehole method

If pre-existing bore-/ inspection holes do not exist in a dam, drilling new ones might not be economically viable or desirable from a structural standpoint. Combining this method with a tracer method could be desirable to gain more information from a single borehole.

#### 4.2.3 Single well technique / point dilution method

This method is faced with the same challenges as the pump- / borehole method. Single well technique does have the benefit of being able to detect flow direction and where in a water filled borehole the flow occurs (high up or low down). This could possibly be used to detect damage inside dams. Whether or not measuring  $K$  with this method is viable in an embankment dam is debatable. The method has more potential for delineation of leakage pathways in dams (Dong et al., 2016)

#### 4.2.4 Quantitative determination of hydraulic conductivity using tracers

The method itself is non-destructive but does require a release point for the tracer. If water level pipes in the dam are already installed these can be used, if not other methods such as a drive point dispersal could be interesting to investigate. A tracer could be released in the water upstream of the dam, either in the general water body or in direct contact with the dam body. If this would work to determine the  $K$  of the dam is not known.

This method has more potential and has been used to detect leakage pathways in dams (Dong et al., 2016).



### 4.3 The primary determining characteristic of hydraulic conductivity

#### 4.3.1 Grain size distribution and pore geometry

Porosity does not determine the  $K$  of a material but the pore geometry might. Not only affect the  $K$ -value directly through longer more complicated flow paths but also by altering the flow velocities (Bağcı et al., 2014). How this translates to a coarse rockfill material where the pore geometry will always be irregular is uncertain.

#### 4.3.2 Compaction and particle movement

It has been found that compaction has an effect on  $K$  (Dan et al., 2016; Zou et al., 2013), an argument can be made that achieving and maintaining the same compaction rate in laboratory tests as the field conditions of the sample tested, is important if representative measurements are to be achieved. If these circumstances are not met or the field conditions are not known, the measured  $K$  can not be assumed to be the same in the field.

#### 4.3.3 Flow regime

It has been concluded that the flow regime does have an effect on the  $K$ -value of a material (Bağcı et al., 2014). It has also been shown that turbulent or transitional flow can occur at low hydraulic gradients and flow velocities (Hansen, 1992; Leibundgut et al., 2009; Sedghi-Asl et al., 2014). The pore geometry can have an impact on the flow velocity and as a result the flow regime during testing (Bağcı et al., 2014). This means that checking for flow regime in testing is important and using the appropriate equations.

Since turbulent or transitional flow has a higher flow velocity at the solid-liquid interface, this will have an impact on particle transport and erosion.

## 5. Topics for future work

- Construct grain size distribution vs hydraulic gradient vs flow velocity diagrams based on real tests.
- Investigate how the transition between different flow regimes affects  $K$  and how the grain size distribution affects the hydraulic gradient at which the flow regimes change.
- Runs tests in a fixed wall permeameter with added one directional compression through the top porous disc. Conduct tests using equipment to monitor movement of the sample and compression rate to investigate how a sample changes under hydraulic load and one directional compression.
- Conduct further field tests using tracers for delineation of leakage pathways.

## 6. Conclusion & recommendations

Several different laboratory and field methods are available for determining hydraulic conductivity,  $K$  and saturated hydraulic conductivity,  $K_s$ . Common for all of these are the controlling characteristics for  $K$ , grain size distribution, pore geometry, degree of compaction, particle movement and flow regime. These characteristics need to be considered when testing in order to produce measurements useful in the field or to process the data correctly. My recommendations are:

- Check for a linear/ non-linear relationship between hydraulic head and flow velocity to determine flow regime. If a linear regime is not found, Darcy's law is not valid.
- In a fixed wall permeameter, calculate  $K_s$  by measuring the pressure drop over the test material only.
- According to this literature study the fixed wall permeameter is the most suitable laboratory method for determining the  $K_s$  in coarse grained materials.
- Tracer methods are suitable for leakage pathway delineation inside embankment dams.
- A sudden divergence from the trendline can be caused by particle movement during testing.

## References

- Angulo-Jaramillo, R., Bagarello, V., Iovino, M., Lassabatere, L., 2016. Infiltration Measurements for Soil Hydraulic Characterization. Springer International Publishing, Lyon.  
<https://doi.org/10.1007/978-3-319-31788-5>
- Ankeny, M.D., Ahmed, M., Kaspar, T.C., Horton, R., 1991. Simple Field Method for Determining Unsaturated Hydraulic Conductivity. *Soil Sci. Soc. Am. J.* 55, 467.  
<https://doi.org/10.2136/sssaj1991.03615995005500020028x>
- Bagarello, V., Iovino, M., Tusa, G., 2000. Factors Affecting Measurement of the Near-Saturated Soil Hydraulic Conductivity. *Soil Sci. Soc. Am. J.* 64, 1203–1210.  
<https://doi.org/10.2136/sssaj2000.6441203x>
- Bağcı, Ö., Dukhan, N., Özdemir, M., 2014. Flow Regimes in Packed Beds of Spheres from Pre-Darcy to Turbulent. *Transp. Porous Media* 104, 501–520.  
<https://doi.org/10.1007/s11242-014-0345-0>
- Behrens, H., Beims, U., Dieter, H., Dietze, G., Eikmann, T., Grummt, T., Hanisch, H., Henseling, H., Käß, W., Kerndorff, H., Leibundgut, C., Müller-Wegener, U., Rönnefahrt, I., Scharenberg, B., Schleyer, R., Schloz, W., Tilkes, F., 2001. Toxicological and ecotoxicological assessment of water tracers. *Hydrogeol. J.* 9, 321–325. <https://doi.org/10.1007/s100400100126>
- Benamar, A., Correia dos Santos, R.N., Bennabi, A., Karoui, T., 2019. Suffusion evaluation of coarse-graded soils from Rhine dikes. *Acta Geotech.* 14, 815–823.  
<https://doi.org/10.1007/s11440-019-00782-1>
- Benson, C.H., Yesiller, N., 2016. Variability of Saturated Hydraulic Conductivity Measurements Made Using a Flexible-Wall Permeameter. *Geotech. Test. J.* 39, 20150138.  
<https://doi.org/10.1520/GTJ20150138>
- Bodeving, L., 2020. Inferring runoff generation processes in a discontinuous permafrost catchment in the northern Sweden using hydrometric, isotopic, and modeling methods. Department of Physical Geography Stockholm University, Stockholm.
- Bordier, C., Zimmer, D., 2000. Drainage equations and non-Darcian modelling in coarse porous media or geosynthetic materials. *J. Hydrol.* 14.
- Castiglione, P., Shouse, P.J., Mohanty, B.P., van Genuchten, M.Th., 2005. Analysis of Temperature Effects on Tension Infiltrometry of Low Permeability Materials. *Vadose Zone J.* 4, 481–487.  
<https://doi.org/10.2136/vzj2004.0134>
- Chapuis, R.P., 2012. Predicting the saturated hydraulic conductivity of soils: a review. *Bull. Eng. Geol. Environ.* 71, 401–434. <https://doi.org/10.1007/s10064-012-0418-7>
- Dan, H.-C., He, L.-H., Xu, B., 2016. Experimental Investigation on Non-Darcian Flow in Unbound Graded Aggregate Material of Highway Pavement. *Transp. Porous Media* 112, 189–206.  
<https://doi.org/10.1007/s11242-016-0640-z>
- Daniel, D.E., Anderson, D.C., Boynton, S.S., 1985. Fixed-Wall Versus Flexible-Wall Permeameters. *Hydraul. Barriers Soil Rock*. <https://doi.org/10.1520/STP34573S>
- David Suits, L., Sheahan, T., Yeung, A., Sadek, S., 2005. Apparatus Induced Error in Hydraulic Conductivity Measurement Using a Lucite® Fixed Wall Permeameter. *Geotech. Test. J.* 28, 12527. <https://doi.org/10.1520/GTJ12527>
- Dong, H., Chen, J., Li, X., 2016. Delineation of leakage pathways in an earth and rockfill dam using multi-tracer tests. *Eng. Geol.* 212, 136–145. <https://doi.org/10.1016/j.enggeo.2016.08.003>
- Eusufzai, M.K., Fujii, K., 2012. Effect of Organic Matter Amendment on Hydraulic and Pore Characteristics of a Clay Loam Soil. *Open J. Soil Sci.* 2, 372–381.
- Ferdos, F., Wörman, A., Ekström, I., 2015. Hydraulic Conductivity of Coarse Rockfill used in Hydraulic Structures. *Transp. Porous Media* 108, 367–391.  
<https://doi.org/10.1007/s11242-015-0481-1>
- Filters for Embankment Dams Best Practices for Design and Construction, 2011. . Federal Emergency Management Agency.
- Hansen, D., 1992. The behavior of flowthrough rockfill dams (Dissertation). University of Ottawa, Ottawa.
- Hartmann, A., Weiler, M., Blume, T., 2020. The impact of landscape evolution on soil physics: evolution of soil physical and hydraulic properties along two chronosequences of proglacial

- moraines. *Earth Syst. Sci. Data* 12, 3189–3204. <https://doi.org/10.5194/essd-12-3189-2020>
- Hölting, B., Coldewey, W.G., 2019. *Hydrogeology*, 1st ed. 2019. ed, Springer Textbooks in Earth Sciences, Geography and Environment. Springer Berlin Heidelberg : Imprint: Springer, Berlin, Heidelberg. <https://doi.org/10.1007/978-3-662-56375-5>
- Jamin, P., Cochand, M., Dagenais, S., Lemieux, J.-M., Fortier, R., Molson, J., Brouyère, S., 2020. Direct measurement of groundwater flux in aquifers within the discontinuous permafrost zone: an application of the finite volume point dilution method near Umiujaq (Nunavik, Canada). *Hydrogeol. J.* 28, 869–885. <https://doi.org/10.1007/s10040-020-02108-y>
- Joel, A., Messing, I., 2000. Application of two methods to determine hydraulic conductivity with disc permeameters on sloping land: Hydraulic conductivity measurements on sloping land. *Eur. J. Soil Sci.* 51, 93–98. <https://doi.org/10.1046/j.1365-2389.2000.00281.x>
- Kandalai, S., Singh, P.N., Singh, K.K., 2018. Permeability of granular soil employing flexible wall permeameter. *Arab. J. Geosci.* 11, 28. <https://doi.org/10.1007/s12517-017-3352-y>
- Koohmishi, M., Palassi, M., 2018. Effect of gradation of aggregate and size of fouling materials on hydraulic conductivity of sand-fouled railway ballast. *Constr. Build. Mater.* 167, 514–523. <https://doi.org/10.1016/j.conbuildmat.2018.02.040>
- Lagerlund, J., 2020. Bestämning av hydraulisk konduktivitet med storskalig permeameter (Metodbeskrivning). Vattenfall AB, R&D, Civil Engineering.
- Leibundgut, C., Maloszewski, P., Külls, C., 2009. *Tracers in hydrology*. Wiley-Blackwell, Chichester, UK ; Hoboken, NJ.
- Luo, Q., Liu, M., Wang, T., Wu, P., 2020. Correction Method for Hydraulic Conductivity Measurements Made Using a Fixed Wall Permeameter. *Math. Probl. Eng.* 2020, 1–9. <https://doi.org/10.1155/2020/1274728>
- Maldaner, C.H., Quinn, P.M., Cherry, J.A., Parker, B.L., 2018. Improving estimates of groundwater velocity in a fractured rock borehole using hydraulic and tracer dilution methods. *J. Contam. Hydrol.* 214, 75–86. <https://doi.org/10.1016/j.jconhyd.2018.05.003>
- Marshak, S., 2015. *Earth: portrait of a planet*, Fifth edition. ed. W.W. Norton & Company, New York.
- Masaoka, N., Kosugi, K., 2018. Improved evaporation method for the measurement of the hydraulic conductivity of unsaturated soil in the wet range. *J. Hydrol.* 563, 242–250. <https://doi.org/10.1016/j.jhydrol.2018.06.005>
- Mohanty, B.P., Kanwar, R.S., Everts, C.J., 1994. Comparison of Saturated Hydraulic Conductivity Measurement Methods for a Glacial-Till Soil. *Soil Sci. Soc. Am. J.* 58, 672–677. <https://doi.org/10.2136/sssaj1994.03615995005800030006x>
- Paiva, C., Ferreira, M., Ferreira, A., 2015. Ballast drainage in Brazilian railway infrastructures. *Constr. Build. Mater.* 92, 58–63. <https://doi.org/10.1016/j.conbuildmat.2014.06.006>
- Part 2: Water permeability tests in a borehole using open systems (ISO 22282-2:2012) (Svensk Standard SS-EN ISO No. SS-EN ISO 22282-2:2012), 2012. , Geotechnical investigation and testing – Geohydraulic testing. Swedish Standards Institute, Stockholm.
- Part 11: Permeability tests (ISO 17892-11:2019) (Svensk Standard SS-EN ISO No. SS-EN ISO 17892-11:2019), 2019. , Geotechnical investigation and testing – Laboratory testing of soil. Swedish Standards Institute, Stockholm.
- Peters, A., Durner, W., 2008. Simplified evaporation method for determining soil hydraulic properties. *J. Hydrol.* 356, 147–162. <https://doi.org/10.1016/j.jhydrol.2008.04.016>
- Peters, A., Durner, W., 2006. Improved estimation of soil water retention characteristics from hydrostatic column experiments: Estimation of Water Retention Characteristics. *Water Resour. Res.* 42. <https://doi.org/10.1029/2006WR004952>
- Reynolds, W.D., Elrick, D.E., 1986. A Method for Simultaneous In Situ Measurement in the Vadose Zone of Field-Saturated Hydraulic Conductivity, Sorptivity and the Conductivity-Pressure Head Relationship. *Groundw. Monit. Remediat.* 6, 84–95. <https://doi.org/10.1111/j.1745-6592.1986.tb01229.x>
- Reynolds, W.D., Lewis, J.K., 2012. A drive point application of the Guelph Permeameter method for coarse-textured soils. *Geoderma* 187–188, 59–66. <https://doi.org/10.1016/j.geoderma.2012.04.004>
- Samingan, A.S., Leong, E.-C., Rahardjo, H., 2003. A flexible wall permeameter for measurements of water and air coefficients of permeability of residual soils. *Can Geotech* 40, 559–574.

- Sedghi-Asl, M., Rahimi, H., Salehi, R., 2014. Non-Darcy Flow of Water Through a Packed Column Test. *Transp. Porous Media* 101, 215–227. <https://doi.org/10.1007/s11242-013-0240-0>
- Siddiqua, S., Blatz, J.A., Privat, N.C., 2011. Evaluating Turbulent Flow in Large Rockfill. *J. Hydraul. Eng.* 137, 1462–1469. [https://doi.org/10.1061/\(ASCE\)HY.1943-7900.0000442](https://doi.org/10.1061/(ASCE)HY.1943-7900.0000442)
- Sidiropoulou, M.G., Moutsopoulos, K.N., Tsihrintzis, V.A., 2007. Determination of Forchheimer equation coefficients a and b. *Hydrol. Process.* 21, 534–554. <https://doi.org/10.1002/hyp.6264>
- Soil Survey Technical Note 6 | NRCS Soils [WWW Document], n.d. URL [https://www.nrcs.usda.gov/wps/portal/nrcs/detail/soils/ref/?cid=nrcs142p2\\_053573](https://www.nrcs.usda.gov/wps/portal/nrcs/detail/soils/ref/?cid=nrcs142p2_053573) (accessed 3.10.21).
- Sridhar, G., Robinson, R.G., 2013. Flexible Wall Permeameter to Measure the Hydraulic Conductivity of Soils in Horizontal Direction. *Geotech. Test. J.* 36, 20120039. <https://doi.org/10.1520/GTJ20120039>
- Statens vattenfallsverk, 1988. Jord- och stenfyllningsdammar. Vattenfall, Stockholm.
- Tennakoon, N., Indraratna, B., Rujikiatkamjorn, C., Nimbalkar, S., Neville, T., 2012. The Role of Ballast-Fouling Characteristics on the Drainage Capacity of Rail Substructure. *Geotech. Test. J.* 35, 104107. <https://doi.org/10.1520/GTJ104107>
- Tuli, A., Denton, M.A., Hopmans, J.W., Harter, T., Mac Intyre, J.L., 2001. Multistep outflow experiment: From soil preparation to parameter estimation. *Hydrol. Dep. Land Air Water Resour. Univ. Calif. Davis* 120.
- What is Embankment Dam? Its Types and Components., 2018. URL <https://civilseek.com/embankment-dam/> (accessed 4.12.21).
- Zou, Y.-H., Chen, Q., He, C.-R., 2013. A new large-scale plane-strain permeameter for gravelly clay soil under stresses. *KSCE J. Civ. Eng.* 17, 681–690. <https://doi.org/10.1007/s12205-013-0217-0>

### Internet resources

- Bear, J., 2013. Dynamics of Fluids in Porous Media. [https://app-knovel-com.ezproxy.its.uu.se/web/toc.v/cid:kpDFPM000I/viewerType:toc/root\\_slug:dynamics-fluids-in-porous?kpromoter=federation](https://app-knovel-com.ezproxy.its.uu.se/web/toc.v/cid:kpDFPM000I/viewerType:toc/root_slug:dynamics-fluids-in-porous?kpromoter=federation) [2021-04-06]
- Chesworth, W., Arbestain, M.C., Macías, F., Spaargaren, O., Mualem, Y., Morel-Seytoux, H.J., Horwath, W.R., Almendros, G., Grossl, P.R., Sparks, D.L., Fairbridge, R.W., Singer, A., 2021. Conductivity, Hydraulic. Springer Link. [https://link-springer-com.ezproxy.its.uu.se/referenceworkentry/10.1007%2F978-1-4020-3995-9\\_125](https://link-springer-com.ezproxy.its.uu.se/referenceworkentry/10.1007%2F978-1-4020-3995-9_125) [2021-03-10]
- D18 Committee. Test Methods for Measurement of Hydraulic Conductivity of Saturated Porous Materials Using a Flexible Wall Permeameter. ASTM International. <https://doi.org/10.1520/D5084-16A> [2021-03-18]
- D18 Committee. Test Method for Measurement of Hydraulic Conductivity of Porous Material Using a Rigid-Wall, Compaction-Mold Permeameter. ASTM International. <https://doi.org/10.1520/D5856-15> [2021-03-18]
- Soil Survey Technical Note 6 | NRCS Soils [https://www.nrcs.usda.gov/wps/portal/nrcs/detail/soils/ref/?cid=nrcs142p2\\_053573](https://www.nrcs.usda.gov/wps/portal/nrcs/detail/soils/ref/?cid=nrcs142p2_053573) [2021-03-10]
- What is Embankment Dam? Its Types and Components., 2018. <https://civilseek.com/embankment-dam/> [2021-04-12]

### Personal communication

- Lagerlund, J., Senior R&D Engineer at Vattenfall, Älvkarlebylaboratoriet (2021). E-mail communication in april.



